CA9700217

RECENT TECHNOLOGICAL DEVELOPMENTS IN ACCELERATING STRUCTURES

Y. Yamazaki
National Laboratory for High Energy Physics (KEK)
1-1 Oho, Tsukuba-shi, Ibaraki-ken 305, Japan

Abstract

A variety of high-β accelerating structures for both proton and electron accelerators are reviewed from modern points of view. Both standing- and traveling-wave structures are discussed. Beam stability is one of the most important factors which must be taken into account regarding modern accelerators in which the beam intensity is an issue.

Introduction

In this report we simultaneously discuss recent developments concerning high-β accelerating structures for electron linacs, high-energy proton linacs and electron rings, since the structures and/or techniques developed for one type of accelerator can sometimes be applied to another. Development has been promoted by the requirement for high-energy, -intensity, and -brightness beams. The following examples of this kind of advanced accelerator are given: electron linacs for TeV colliders, electron linacs for free-electron lasers, electron rings for B-factories, and proton linacs for meson factories or spallation neutrons, including those used for transmutation. The typical parameters are listed in Table I.

TABLE I
Examples of Future Proton Linacs, Electron Linacs and Electron Rings

Parameters of JHP proton linac [1], OMEGA proton linac [2], Japan's linear collider [3], Los Alamos Advanced FEL linac [4], and KEK B factory [5].

Accelerator		Energy	Peak Current	Average Current	Emittance (90%, norm)	Length
JHP	H^-	1 GeV	20 mA	400 μA	1π mmmr	0.4 km
OMEGA	p	1.5 GeV	100 mA	10 mA	6π mmmr	1.2 km
JLC	e	500 GeV	1.4 A	6 μA	0.3π mmmr	12 km
A-FEL	e	20 MeV	6 A	6 mA	9πmmmr	
KEK B	e	3.5 GeV	2.6 A	2.6 A		1.5 km

The ideal accelerating field is axially symmetric and longitudinally formed as designed. (It is longitudinally periodic in electron accelerators.) The field should be pure both transversely and longitudinally, being free from any field error. Although the peak beam currents (the beam current within a beam pulse) in proton linacs are significantly lower than those in electron accelerators (see Table I), a high degree of longitudinal field purity is required in high-intensity, high-energy proton linacs. We first give the reasons for this, and then discuss longitudinal field stability in terms of beam loading and structural imperfections. A discussion concerning the power efficiency of various structures follows, since the alternating-perodic structure (APS) [6], sometimes referred to as a bi-periodic structure, plays an important role regarding both field stability and power efficiency. We then discuss transverse field purity (or axial symmetry).

Even if an ideal accelerating field were to be efficiently provided, the structure would still not be perfect. It should also be free from beam blowup (BBU) [7,8] in linacs or beam instabilties [9-11] in rings. The last section discusses efforts being made to cure BBU or instabilities.

Effect of the Longitudinal Field Purity on Electron and Proton High-β Accelerators

The longitudinal field purity is particularly important in high-intensity, high-energy proton linacs for the following reason. The beam loss of high-energy protons should be eliminated, for example, down to an order of 10^{-3} to 10^{-5}, since it generates high radioactivity during long-term operation. A beam loss of this order arises from the tail or halo, the generation mechanism of which has not yet been elucidated either theoretically or empirically. It is quite possible that slight field errors give rise to the tail, halo, or emittance growth in cooperation with non-linear forces, which arise from a space-charge effect or non-linearity in the phase oscillation, itself. It is noted here that the synchrotron oscillation wavelength in a proton linac is of the order of the tank length. If the field error has some Fourier component of the synchrotron wavelength, a slight field error in a tank, for example field tilt or droop, could increase the amplitude of the synchrotron oscillation. For example, a simulation [12] indicated that phase droops of ± 3° in 8-m tanks generated some loss of the beam situated in the fringe of the longitudinal phase space during its excursion through the JHP linac. This is a cooperative phenomenon of the field error and non-linear phase oscillation.

In electron rings the synchrotron wavelengths are extremely longer than cavity lengths. Nevertheless, longitudinal field stability is also important in electron rings. Since the synchrotron frequency is a critical parameter in operating high-intensity, high-energy electron rings in order to maintain a large dynamic aperture, the accelerating field should be accurately controlled, requiring high field stability in a multi-cell cavity. This is the reason why we chose the APS for the TRISTAN main ring [13-16], rather than the π-mode cavities being used for PETRA, PEP or LEP.

Field Stability or Longitudinal Field Purity

Longitudinal field errors are introduced by beam loading or structual imperfections. The field stability against the effect of structural imperfections is characterized in terms of the following [17-19]:

$$N\Delta_a \equiv \Delta f_a/(\Delta f_p/2N),$$
$$N\Delta_c \equiv \Delta f_c/(\Delta f_p/2N),$$
$$N\delta_a = \delta f_a/(\Delta f_p/2N),$$

and

$$N\delta_c = \delta f_c/(\Delta f_p/2N),$$

where the parameters with suffices a and c are for accelerating cells and coupling cells, respectively. Coupling cells are cells without a field. Parameters Δf_a and Δf_c are cell-frequency errors; $\delta f_a = f_a/(2Q_a)$ and $\delta f_c = f_a/(2Q_c)$ are the half widths of the resonances or the damping rates of the cells. The denominator of $\Delta f_p/2N$, with a passband width of Δf_p and N being the number of accelerating cells, is the frequency difference between the accel-

erating mode and the neighboring mode. It is noted that all of the parameters are normalized by $\Delta f_p/2N$, implying that the field is more stable for large coupling, that is, a wide passband. The parameter $N\delta_a$ is nothing but the attenuation parameter in the case of the $\pi/2$ traveling-wave mode.

In a steady state the field stability of traveling-wave (TW) operation (phase shift from cell to cell is Φ) is given by [20]

$$\delta x_a/x_a = j(1/2)(1/\sin\Phi)(N\Delta_a),$$

while those of the standing-wave (SW) operation are summarized in Table II [17-19]. Here, the parameter x_a is the average of the square root of the stored energy in an accelerating cell, while δx_a and δx_c are the maximum values among errors in the square roots of the stored energies in the accelerating and coupling cells, respectively. The parameter [19]

$$\delta_t = \delta_a (1 + P_b/P_c)$$

that appears in Table II is introduced in order to take into accout the beam loading effect, where P_b and P_c are the beam loading and power dissipation, respectively.

Table II
Maximum Deviation $\delta x_a^{(i)}$ of the i-th Term in Square Roots of Stored Energies in Accelerating Cells and Maximum Value $\delta x_c^{(i)}$ of the i-th Term in Those in Coupling Cells

Consider Δa and Δ_c as positive in this table. Terms to which a symbol j is attached represent phase diviations in radian. If tuners are installed at every M accelerating cells (the number of the tuners is N/M), $N\Delta_a$ should be replaced by $M\Delta_a$. The values for the π mode can be obtained by setting $\delta_c = 0$ and $\Delta_c = 1/2$ in the $\pi/2$ mode.

mode ϕ	$\pi/2$	$2\pi/3$
$\delta x_c^{(1)}/x_a$	$N\Delta_a$	$N\Delta_a$
$\delta x_c^{(2)}/x_a$	$jN\delta_t$	$jN\delta_t$
$\delta x_a^{(1)}/x_a$	$(1/2)(N\Delta_c)(N\Delta_a)$	$(1/4)(N\Delta_c)(N\Delta_a)$
$\delta x_a^{(2)}/x_a$	$(1/4)(N\delta_c)(N\delta_t)$	$(1/8)(N\delta_c)(N\delta_t)$
$\delta x_a^{(3)}/x_a$	$j(1/2)(N\delta_c)(N\Delta_a)$	$j(1/4)(N\delta_c)(N\Delta_a)$
$\delta x_a^{(4)}/x_a$	$j(1/4)(N\Delta_c)(N\delta_t)$	$j(1/8)(N\Delta_c)(N\delta_t)$
$\delta x_a^{(5)}/x_a$	—	$(1/2)N\Delta_a$
$\delta x_a^{(6)}/x_a$	—	$jN\delta_t$

Under TW operation the amplitude attenuation arising from wall loss is taken into account in the design stage, no matter which of the constant-gradient, constant-impedance or detuned structures is chosen. Under SW operation it is usual to consider the field droop due to the wall loss or beam loading as a kind of field error, although the droop can be compensated for by adjusting the coupling coefficients, such as the constant-gradient TW structure. Under either TW or SW operation the manufacturing error in the coupling coefficient gives further rise to some amplitude deviation from the designed value.

It can be seen that the effect of the manufacturing error is of the first order on the field stability under steady-state TW operation; it is of the second order under $\pi/2$ SW operation. If the structure is used in the steady state, $\pi/2$ mode SW operation is advantageous over TW operation regarding field stability.

Power Efficiency or Shunt Impedance

The steady-state power efficiency of the SW structure is also better than that of the TW structure [21] if the proper structure is chosen. Here, the SW structure is referred to as a structure which is suitable for SW operation, while the TW structure is suitable for TW operation. We now consider the disc-loaded structure shown in Fig. 1 a). It should be noted that the shunt impedance of the π-mode is the same for both the TW and SW modes, since the difference between TW and SW vanishes under π-mode operation. (Throughout this paper we deal with the shunt impedance, which includes the transit time factor.) It is true that the shunt impedance of the $\pi/2$ SW mode is half that of the $\pi/2$ TW mode in the case of a uniformly periodic structure (Fig. 1 a)), since the field vanishes in half of the cells under SW operation. (In other phase-shift SW modes the phase difference between the beam and the field is accumulated from one cell to another, halving the shunt impedance together with the effect of a non-field cell.) However, cells without a field (coupling cells) can be shortened, as shown in Fig. 1 b), if one wishes to recover the shunt impedance. This is how the alternating-periodic structure (APS) was invented [6]. In other words, the APS is a structure with both the π-mode shunt impedance and the $\pi/2$-mode field stability; a structure of this type is referred to as an on-axis coupled structure (OCS). Although a triperiodic structure [22] operated in the $2\pi/3$ mode was proposed in order to further improve the shunt impedance by eliminating one out of two couplig cells, the field stability becomes worse, as shown in Table II [19].

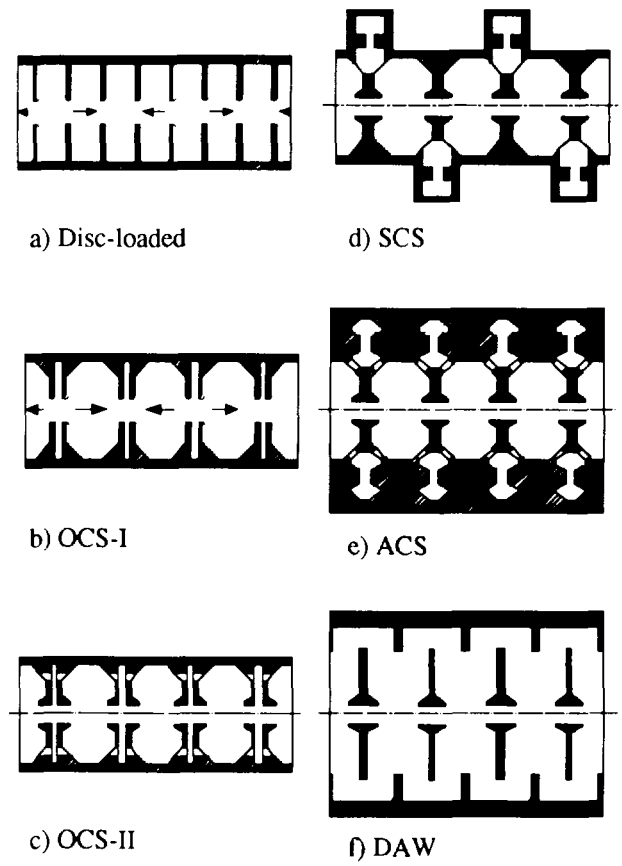

Fig. 1 $\pi/2$-mode standing-wave structures

At this point the TW is still advantageous over the SW, since the $2\pi/3$-mode shunt impedance used in the TW is about 40

percents higher than that of the π-mode. Equipment with nose cones [23], as shown in Fig. 1 c), increases the impedance by typically 30 percent (β~1) or 100 percent (β~0.5) according to a SUPERFISH [24] calculation. However, since the electrical coupling through a beam hole is almost eliminated by attaching the nose cones, coupling slots are required in order to restore the coupling coefficient. The coupling slots partly cancel any increase in the shunt impedance by an order of ten percent, blocking current flow in a disc. (Although the effect of the coupling slots on the shunt impedance is primarily dependent upon the coupling coefficient, it is also dependent upon the detailed form of the coupling slots.) On the other hand, some power in the TW mode (nearly 20 percent) goes out of the last cell, unless the power is recirculated to the first cell, as in a resonant ring. An on-axis coupled structure with nose cones and coupling slots has approximately the same power efficiency as does the TW structure. (Some people may criticize the fact that the structure shown in Fig. 1 c) is no longer literally an on-axis coupled structure. However, this terminology is not only historical, but it also implies that coupling cells are located on-axis. The notation on the geometrical form of APS refers to the location of coupling cell.)

On-axis coupling cells still occupy and consume the space on the beam axis, which can otherwise be used for acceleration. A coupling cell, ideally having no field or nothing to do with acceleration, can have various forms as long as it maintains the field-stabilizing function. The side-coupled structure (SCS) [25,17] was invented by displacing coupling cells to the "side" (Fig. 1 d)). In this way the geometrical form of the accelerating cell can be optimized in order to obtain the highest shunt impedance. However, axial symmetry is lost.

Since axial symmetry is important for a high-intensity accelerator, as discussed in the next section, we developed an annular-ring coupled structure (ACS) [26,27] in order to recover axial symmetry. It is noted that the ACS can be topologically obtained by rotating the SCS around the beam axis, as shown from Fig. 1 e). However, we had a difficult time to put the structure into practical use, since the coaxial coupling cells of the ACS have many higher-order modes just above the coupling mode. (Note that the higher-order modes are localized in the coupling cells, causing no direct harm to the beams.) It had been reported [27] that a serious depression in the quality factor arises from excitation of the coupling-cell quadrupole mode. We understood that the excitation arises from an alternative orientation of two coupling slots. Also, the two coupling slots decrease the frequency of one of the dipole modes in the coupling cells down to the accelerating passband [28]. We anticipated that both these problems would be solved by recovering axial symmetry, which is also advantageous regarding the field purity as discussed in the next section. The problems were actually solved by using four or eight coupling slots [29]. If one uses a coupling of 5 percent, the coupling slots deteriorate the quality factor by 17 percent, which is 1.5 times larger than in the SCS case. In order to obtain the same coupling, the ACS requires larger slots than does SCS, since the axially symmetrized coupling cells of the ACS are larger than those of the SCS. Since the ACS became quite promising for practical use, we constructed 1296-MHz high-power models [30,31] with two five-cell tanks connected by a five-cell bridge coupler [32]. The models were tested up to 6.5 MV/m, which is 1.5 times higher than the power level necessary for the JHP linac (600 μs, 50 Hz).

The disc-and-washer (DAW) structure [26] shown in Fig. 1 f) was at first appreciated for its extremely high shunt impedance and extremely high coupling. There were, however, two difficult problems to solve: the washers must be supported by stems, and the passband of a transverse dipole mode crosses the accelerating mode. Solutions to the former are partly associated with a decrease in the quality factor. The latter problem was solved by pushing up the frequency of the transverse mode [33]; again, however, this was associated with a decrease in its Q value. The other solution is to produce a stopband of the transverse mode in the vicinity of the accelerating mode [34]. The DAW of the first type was beam-tested in the TRISTAN accumulator ring [33], while the latter was recently tested at the INR meson factory in Moscow. It is noted that the DAW is advantageous over any other structure due to its extremely high coupling.

The shunt impedances of the various structures measured in different laboratories are sometimes difficult to compare, since they can be increased by decreasing the following parameters: the bore radius, disc thickness, nose-cone angle, and nose-cone radius shown in Fig. 2. (The frequency (f) dependence can be scaled by using its $f^{1/2}$-law, if the compared structures have the same figure.) An approximate comparison is given in Table III, where the shunt impedance is normalized by a π-mode shunt impedance, thus being optimized while holding the above parameters fixed.

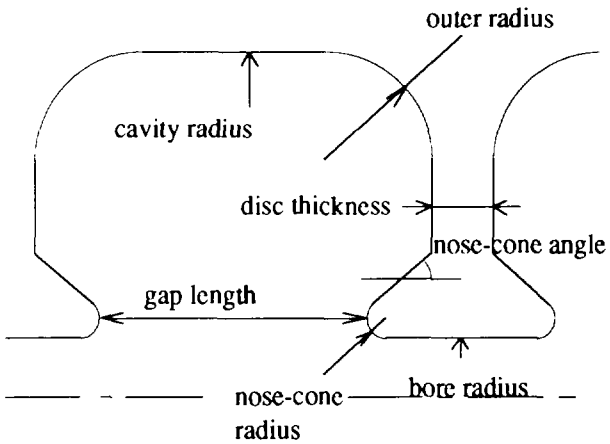

Fig. 2 Parameters which determine the sunt impedance

TABLE III
Approximate Comparison of Shunt Impedances

The shunt impedances are normalized by the optimized π-mode shunt impedance. The OCS-I is an OCS without nose cones or coupling slots, while the OCS-II is one with nose cones and coupling slots. The shunt impedances of the OCS-II can be increased up to 0.9, if one uses a thin disc and a small coupling cell. (A coupling of 5 % except for the OCS-I and DAW.)

β	OCS-I	OCS-II	SCS	ACS	DAW [35]
0.9	~0.6	~0.7	~0.88	~0.83	~0.95
0.5	~0.3	~0.5	~0.88	~0.83	~0.91

Transverse Field Purity or Axial Symmetry

In the preceding section we discussed the longitudinal field purity. In this section we deal with the axial asymmetry in the accelerating field. One can classify the axial asymmetry in terms of the multiplicity: if an asymmetry has a component of $\sin m\phi$, where ϕ is the azimuthal angle, we refer to the asymmetry

as being 2^m-pole. Although the effect of the axial asymmetry of the accelerating field has not been fully studied quantitatively, partly because of a lack of experimental data, we believe that the axial symmetry of the accelerating field is important for a high-intensity accelerator. The presence of the dipole component in the accelerating field implies that the beam is kicked by the acceleration, giving rise to a coupling of the betatron oscillation with the synchrotron oscillation. In rings it should increase the undesirable effects of synchro-betatron resonances, while in linacs it should again give rise to emittance growth under some non-linear forces. It was recently observed that the quadrupole component gives rise to emittance growth through its interaction with the solenoid field in the electron linac for FEL [4].

If a cavity has axial asymmetry geometrically, the asymmetry mixes the otherwise symmetric accelerating mode with multipole modes. The amplitude of the mixing is proportional to the asymmetry and the product of field strengths of the two modes there, and inversely proportional to the frequency difference between the accelerating mode and multipole modes. This is essentially the same mechanism as in the longitudinal case.

The SCS has dipole asymmetry, the OCS with two coupling slots has quadrupole asymmetry, while the ACS with four coupling slots has octupole asymmetry. Recent estimates [36] have indicated that the accelerating field in the SCS has a dipole component of approximately one percent on the axis. A quadrupole component (E_y/E_z) of around 0.3/m appeared [4] in the accelerating mode of OCS with two coupling slots, where E_y and E_z are the transverse and longitudinal fields, respectively. In contrast, the ACS has a negligibly small octupole component in its accelerating field [36], partly because the frequencies of octupole modes are significantly higher than the dipole or quadrupole modes, and partly because the octupole field is very small near the beam axis. This is the reason why we used an electrically coupled OCS without any coupling slot (Fig. 1 b)) for the TRISTAN rings and developed the ACS for the JHP linac.

The DAW structure is disadvantageous regarding transverse field purity, since the deflecting dipole modes are still situated in the vicinity of the accelerating mode, even if the dipole modes are deviated by either device.

BBU in Linacs and Beam Instabilities in Rings

If the beam traverses through a cavity off axis, the excited deflecting modes (TM1-like modes, or HEM1 modes) give rise to beam blowup (BBU) [7,8], sometimes referred to as beam breakup, in linacs. Modes with low resonant frequencies and with high quality factors mainly deflect the beams in the following bunches, while those with continuum spectra deflect the tail in a bunch. In rings the same mechanism increases the amplitude of betatron oscillation near synchro-betatron resonances [37,38]. In either case the beam axis should be aligned along the "cavity axis" where the deflecting field vanishes in order to suppress the BBU or the effect of synchro-betatron resonances. However, if the cavity is axially asymmetric, the cavity axis in this sense differs from one mode to another, making it impossible to align the beam axis for all modes. This is another undesirable effect of the axial asymmetry of cavities.

More serious in electron rings is that coherent betatron oscillations are induced by deflecting modes, which are, in turn, excited by the oscillations [9]. This phenomenon is referred to as a transverse coupled-bunch instability. In rings, a longitudinal coupled-bunch instability [10] is also excited due to the presence of longitudinal higher-order modes (TM0 modes). Both of the coupled-bunch instabilities were empirically studied in the PF [39-42]. The measured threshold currents were in agreement with the theoretical predictions within a few ten percent [42]. The DAW structure is disadvantageous regarding the BBU or instabilities for the following reasons. Since the operational mode of the DAW is not fundamental, but, rather, a higher-order mode, the DAW has significantly more higher-order modes than do the OCS, ACS and SCS. Even worse is that the characteristics of these higher-order modes in the DAW are very hard to study and/or to understand, compared with those of the other structures.

In linear colliders high-intensity electron beams are accelerated through extremely long linacs; in B factories extremely high currents are accelerated and/or stored. In either case the threshold currents of the BBU or the instabilities must be drastically increased. The first method for curing the BBU or the instabilities is to distribute the resonant frequencies of the higher-order modes in order to avoid any accumulation of the effect over a tank, a linac or a ring. In the case of proton linacs the distribution is automatically realized, though only partly, since the cell length is increased (as a result the cavity diameter also varies), as the beam is accelerated. In the case of electron linacs the bore radius of the constant-gradient structure is decreased down stream of the traveling wave. In modern accelerators the automatic distribution of the resonant frequencies is not sufficient to eliminate the BBU. Thus, the bore radii are varied as effectively as possible in suppressing the BBU, although the gradient becomes only approximately constant, not exactly in this case. This type of TW structure is referred to as a detuned structure [43,44]. In the TRISTAN main ring the radii of the APS cavities are intentionally distributed [16] so that the frequencies of the "dangerous" modes are distributed among the two revolution frequencies, resulting in an approximate cancellation of the excitation of higher-order modes by their damping. (Typical dangerous modes are TM011-like, TM110-like and TM111-like modes.)

The second method used to avoid the BBU or the beam instabilities is to equip a cavity with couplers, through which dangerous higher-order modes are removed and damped by matched loads. The dampers used in the TRISTAN rings decreased the quality factor of the TM111-like modes by more than an order of magnitude, while that of the TM011-like mode by two orders of magnitude [45]. The dampers developed for the PF had better performances to suppress the higher-order modes [46]. Strong electric fields at the wall of the TM011-like and TM111-like modes are relatively easy to couple out, since the accelerating TM010-like mode has no electric field there. On the contrary, the TM110-like mode has only a magnetic field at the wall, similar to the case of the accelerating mode, and is thus difficult to damp without a serious depression of the Q value of the accelerating mode. A "single-mode cavity" (Fig. 3 a)) introduced by Weiland [47] cannot damp the TM110-like mode either, which is the lowest-frequency standing-wave mode originating from the TM11 wave-guide mode. (The single-mode cavity has the lowest impedance at the high-frequency spectra, being the most immune against single-bunch instabilities.)

In order to obtain a "damped cavity" without any higher-order mode, having a reasonable amount of the accelerating shunt impedance, a variety of cavities are being proposed and investigated. The three-dimensional code MAFIA [48] makes it significantly efficient to design this kind of cavity, together with the use of a calculation method of the external Q [49]. This method was independently applied by Gluckstern et al. [50], Kageyama [51] and Kroll et al. [52]. Different concepts were presented by Conciauro et al. [53], Palmer [54], and Kageyama [55], respectively, for a damped cavity (Fig. 3 b)-e)) in which the TM110-like mode is well damped down to a Q value of a few 10 or less. The concepts of Palmer and Conciauro et al. were further improved by KEK B factory group [56] and SLAC B factory group [57],

respectively. Kageyama's concept is being seriously studied by the Cornell B factory group [58,59] with regard to their superconducting cavity. Very recently, Shintake [60] proposed the "choke-mode cavity" shown in Fig. 3 f). Both Palmer's and Shintake's cavities were devised for multi-cell cavities, while the others can be used only for a single-cell cavity. It will be interesting to see which structure survives the next decade, and even more interesting to see new structures being invented.

Conclusions

We must omit any discussion concerning rather technical aspects such as tuning, machining, brazing, cooling, vacuum and so forth in this short report, although these aspects are sometimes more important in choosing a suitable structure. Finally, it is stressed that each structure has its own advantage, and that the best choice is dependent upon the specifications of each machine.

Acknowledgement

The author is grateful to K. Yoshino for his SUPERFISH calculations of shunt impedances.

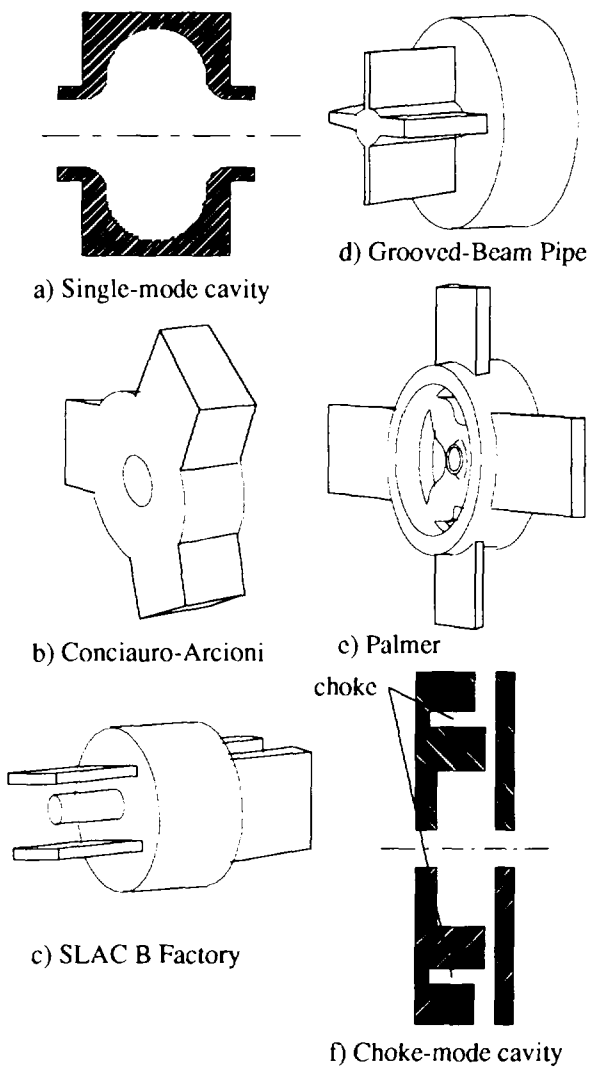

Fig. 3 Damped cavities

References

[1] Y. Yamazaki and M. Kihara, Proc. 1990 Linear Accel. Conf., 543 (1990).
[2] Y. Kaneko, Proc. 2nd Int. Conf. Advances Nuclear Energy Research, Mito, 25 (1990).
[3] K. Takata, KEK Preprint 92-70.
[4] R. L. Sheffield er al., Nucl. Instr. Meth. **A318**, 282 (1992).
[5] S. Kurokawa et. al., KEK Report 90-24 (1991).
[6] T. Nishikawa et al., Rev. Sci. Instr. **37**, 652 (1966).
[7] P. B. Wilson, HEPL-297, Stanford (1963).
[8] R. L. Gluckstern, AADD-38, Brookhaven (1964).
[9] F. J. Sacherer, Proc. 9th Int. Conf. on High Energy Accelerators, 347 (1974).
[10] F. J. Sacherer, IEEE Trans. Nucl. Sci. **NS-20**, 825 (1973).
[11] F. J. Sacherer, IEEE Trans. Nucl. Sci. **NS-24**, 1393 (1977).
[12] T. Kato, private communication.
[13] T. Higo et al., Proc. 5th Symp. Accel. Sci. Tech. 114 (1984).
[14] T. Higo et al., IEEE Trans. Nucl. Sci. **NS-32**, 2834 (1985).
[15] K. Akai et al., Proc. 13th Int. Conf. on High Energy Accelerators 303 (1986).
[16] T. Higo et al., Proc. 1987 IEEE Part. Accel. Conf. 1945 (1987).
[17] E. A. Knapp et al., Rev. Sci. Instr. **39**, 979 (1968).
[18] Y. Yamazaki et al., Part. Accel. **22**, 273 (1988).
[19] Y. Yamazaki, Part. Accel. **32**, 39 (1990).
[20] P. M. Lapostolle and A. L. Septier, Linear Accelerators, North Holland (1970).
[21] R. H. Miller, Proc. 1986 Linac Conf., 200 (1986).
[22] B. Epsztein and Tran Duc Tien, Proc. 1968 Proton Linear Accel. Conf., 457 (1968).
[23] S. O. Schriber et al., Proc. 1972 Proton Linac Conf., 140 (1972).
[24] K. Halbach and R. F. Holsinger, Part. Accel. **7**, 213 (1976).
[25] E. A. Knapp et al., Proc. Linear Accel. Conf., 83 (1966).
[26] V. G. Andreev et al., Proc. 1972 Proton Linac Conf., 114 (1972).
[27] R. K. Cooper et al., Preprint LA-UR-83-95 (Los Alamos National Laboratory).
[28] R. A. Hoffswell and R. M. Laszewski, IEEE Trans. Nucl. Sci. **NS-30**, 3588 (1983).
[29] T. Kageyama et al., Part. Accel. **32**, 33(1990).
[30] T. Kageyama et al., Proc. 1990 Linear Accel. Conf., 150 (1990).
[31] K. Yamasu et al., ibid. 126 (1990).
[32] Y. Morozumi et al., ibid. 153 (1990).
[33] S. Inagaki, Nucl. Instr. Meth. **A251**, 417 (1986).
[34] V. G. Andreev et al., IEEE Trans. Nucl. Sci. **NS-30**, 3575 (1983).
[35] V. G. Andreev, private communication.
[36] T. Kageyama et al., TU4-56 in this conference.
[37] R. M. Sundelin, IEEE Trans. Nucl. Sci., **NS-26**, 3604 (1979).
[38] T. Suzuki, Nucl. Instr. Meth. **A241**, 89 (1985).
[39] Y. Yamazaki et al., KEK 80-8 (1980).
[40] Y. Yamazaki et al., KEK 83-3 (1983).
[41] Y. Yamazaki et al., KEK 83-7 (1983).
[42] H. Kobayakawa et al., Jap. J. Appl. Phys. **25**, 864 (1986).
[43] H. Deruyter et al., SLAC-PUB-5322 (1990). T. Higo, KEK Proceedings 91-10 (1991).
[44] K. A. Thomson and J. W. Wang, Proc. 1991 IEEE Part. Accel. Conf., 431 (1991).
[45] Y. Morozumi et al., Part. Accel. **29**, 85(1990).
[46] Y. Yamazaki et al., IEEE Trans. Nucl. Sci. **NS-28**, 2915 (1981).
[47] T. Weiland, DESY 83-073, 1983.
[48] R. Klatt et al., Proc. 1986 Linac Conf., 276 (1986).
[49] J. C. Slater, Microwave Electronics, Van Nostrand, (1950).
[50] R. L. Gluckstern and R. Li, Proc. 1988 Linac Conf., 357 (1988).
[51] T. Kageyama, KEK Report 89-4, 1989.
[52] N. M. Kroll and D. U. L. Yu, SLAC-PUB-5171 (1990).
[53] G. Conciauro and P. Arcioni, Proc. 2nd European Particle Accelerator Conference, 149 (1990).
[54] R. B. Palmer, SLAC-PUB-4542, 1988.
[55] T. Kageyama, Proc. 8th Symp. Accel. Sci. Tech. 116 (1991).
[56] M. Suetake et al., KEK Report 90-24 (1991), pp. 85.
[57] An Asymmetric B Factory based on PEP Conceptual Design Report (1991).
[58] Berkelman et al., CESR-B Conceptual design for a B factory based on CESR, CLNS-91-1050 (1991).
[59] J. Kirchgessner et al., TU4-55 in this conference.
[60] T. Shintake, to be published in Jpn. J. Appl. Phys. Lett.; KEK Preprint 92-51 (1992).